RSC Advances

PAPER

View Article Online
View Journal | View Issue

Cite this: *RSC Adv.*, 2025, **15**, 1680

Synthesis and antibacterial evaluation of quinoline–sulfonamide hybrid compounds: a promising strategy against bacterial resistance†

Zohaib Saifi,[a] Asghar Ali,[bc] Afreen Inam,[a] Amir Azam,[a] Mohan Kamthan,[c] Mohammad Abid *[b] and Imran Ali*[a]

Antibiotic-resistant bacteria are a serious global health threat, making infections harder to treat and increasing medical costs and mortality rates. To combat resistant bacterial strains, a series of compounds (QS1–12) were synthesized with an excellent yield of 85–92%. Initial assessments of these analogues as potential antibacterial agents were conducted through a preliminary screening against a panel of diverse bacterial strains. The results identified compound QS-3 as the most effective antibacterial candidate, exhibiting exceptional inhibitory activity against *P. aeruginosa* with a minimum inhibitory concentration (MIC) of 64 μg mL^{-1}. Furthermore, QS-3 demonstrated a favorable synergistic effect when combined with ciprofloxacin. Notably, the compound displayed minimal cytotoxicity, inducing less than 5% lysis of red blood cells (RBCs). Significantly, QS-3 exhibited enhanced inhibitory activity, particularly against the antibiotic-resistant strains AA202 and AA290. *In silico* predictions of physicochemical properties underscored the drug-like qualities of the designed compounds. Additionally, molecular docking poses, ligPlot images, and a binding affinity of −8.0 kcal mol^{-1} further reinforced their potential as promising antibacterial agents. Briefly, the reported compound QS3 may be a future broad-range antibacterial agent.

Received 13th July 2024
Accepted 28th November 2024

DOI: 10.1039/d4ra05069j

rsc.li/rsc-advances

1. Introduction

The improper use of limited antibiotics has made the problem much worse, rendering previously curable infections incurable, and the effectiveness of the currently available antibiotics is declining more quickly. As a result, bacterial infections are worsened by rising antibacterial resistance, especially in developing nations with widespread antibiotic access.[1,2] Antibiotic-resistant bacteria contributed to around five million deaths in 2019, with projected mortality expected to rise by 2050. Recognized as a major global threat by the WHO, experts warn we may be entering a "post-antibiotic age". This crisis highlights the urgent need for new, innovative antibacterials to combat infections.[3–5] The combination therapy using multiple antibiotics simultaneously has been a key approach to combat bacterial infections and prevent resistance.[6,7] Augmentin, a combination of amoxicillin and clavulanic acid, uses amoxicillin to disrupt growth while clavulanic acid inhibits β-lactamase enzymes that resist antibiotics.[8,9] Hybrid drugs improve upon combination therapies by merging multiple elements into a single molecule, simplifying administration, reducing side effects, and avoiding drug interactions. This targeted approach enhances efficacy and safety, making hybrid drugs a promising solution for complex conditions.[10,11] For this purpose, we selected two core moieties quinoline and sulfonamides, both have good antibacterial properties. Quinolones, the first class of antibiotics known to inhibit bacterial DNA synthesis, have revolutionized the treatment of bacterial infections. By targeting nucleic acid synthesis and disrupting key enzymes such as DNA gyrase and topoisomerase IV, these compounds effectively hinder bacterial growth.[12] Beyond their antibacterial properties, quinoline derivatives have been extensively explored for diverse pharmacological applications, including cardiovascular, central nervous system (CNS),[13] analgesic,[14] antimalarial,[15] anticancer,[16] antibacterial,[17] antiviral,[18] antifungal,[19] anti-inflammatory, and more[20] Recognizing their critical role in drug development, this study focuses on the gyrase protein (PDB: 3qtd) and employs molecular docking analysis to further understand its interactions with quinolone derivatives. The quinolone moiety forms the backbone of several widely recognized antibiotic drugs, such as ciprofloxacin (i), norfloxacin (ii), sparfloxacin (iii), levofloxacin (iv), moxifloxacin (v), and besifloxacin (vi) (Fig. 1).[21] These medications represent successive generations of fluoroquinolones, each iteration designed to improve potency and therapeutic

[a]*Department of Chemistry, Jamia Millia Islamia, Jamia Nagar, New Delhi-110025, India. E-mail: iali2@jmi.ac.in*

[b]*Department of Biosciences, Jamia Millia Islamia, New Delhi-110025, India. E-mail: mabid@jmi.ac.in*

[c]*Department of Biochemistry, School of Chemical and Life Sciences, Jamia Hamdard, New Delhi-110062, India*

† Electronic supplementary information (ESI) available. See DOI: https://doi.org/10.1039/d4ra05069j

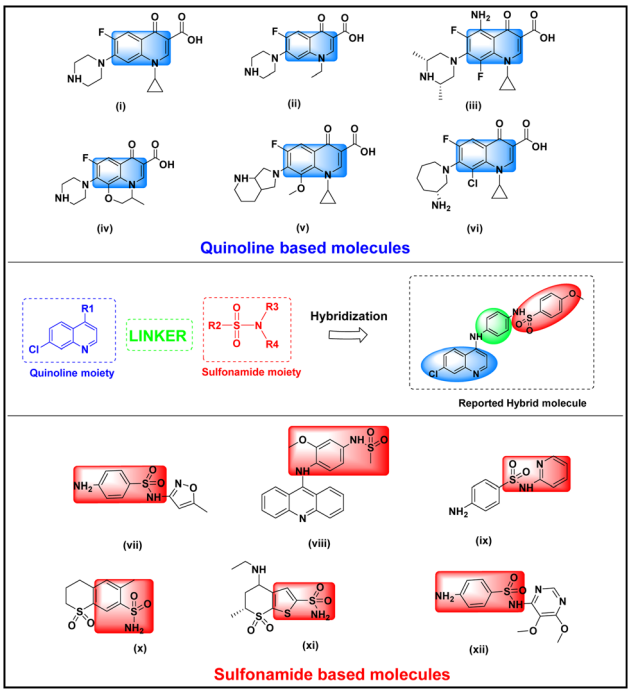

Fig. 1 Rationale design strategy of quinoline–sulfonamides hybrid (a) quinoline and sulfonamide moieties of available drugs matched with red and blue dotted lines, respectively. The linker in green sphere joined quinoline and sulfonamide moieties. The black sphere is a hybrid molecule.

effectiveness. Over time, these advancements have significantly enhanced the clinical utility of quinolones, solidifying their role as critical agents in combating bacterial infections.[22] In recent years, quinolones have been at the forefront of research as powerful antibacterial agents, garnering considerable attention for their potential in addressing infectious diseases. Efforts to develop and optimize these compounds have led to the discovery and synthesis of novel derivatives, showcasing a wide range of promising biological activities. These advancements not only underscore the evolving capabilities of fluoroquinolones but also highlight their crucial role in combating infectious diseases and tackling the growing challenge of antibacterial resistance.[23]

On the other hand, sulfa drugs, renowned in the pharmaceutical industry for their sulfonamide moiety, are widely used to treat various bacterial infections. These compounds exert their antibacterial effects by inhibiting dihydropteroate synthase (DHPS), an essential enzyme in the bacterial folate biosynthesis pathway. This inhibition disrupts bacterial growth and cell division. Notably, this pathway is absent in higher organisms, making it an ideal target for developing effective antibacterial therapies.[24,25] Additionally, they demonstrate antibacterial properties,[26] antifungal capabilities,[27] anti-inflammatory actions,[28] antioxidant qualities,[29] diuretic effects,[30] anticancer properties,[31] interactions with carbonic anhydrases,[32] antitumor potentials,[33] Alzheimer diseases,[34] anti-tubercular activities,[35] anti-diabetic effects,[36] HIV inhibition,[37] antiviral actions,[38] and anti-malarial.[39] Several sulfonamide derivatives are commercially available and widely used as antibacterial drugs. Notable examples include (vii), amsacrine (viii), sulfapyridine (ix), meticrane (x), dorzolamide (xi), sulfadoxine (xii), *etc.* (Fig. 1).[21]

To highlight the importance of this advancement, we explore several examples of quinoline and sulfonamide-based drugs that have demonstrated significant antibacterial properties. This paper presents the synthesis, spectroscopic characterization, and antibacterial activity of novel quinoline–sulfonamide hybrids.

2. Results and discussion

2.1 Chemistry

The availability of access to the title compounds *via* widely available starting materials is a significant advantage of our simple and fast synthesis process. The synthesis of title compounds QS(1–12) is achieved by a synthetic protocol as shown in Scheme 1. The 4,7-dichloroquinoline was condensed with *p*-phenylenediamine/*m*-phenylenediamine in presence of catalyst *p*-TSA to afford the *N*-(7-chloro-quinolinyl-4-yl)-benzene-1,4-diamine QS-(i) or *N*-(7-chloro-quinolinyl-4-yl)-benzene-1,3-diamine QS-(ii).[40] Both these compounds QS(i–ii) were reacted with different substituted benzene sulfonyl chloride at room temperature to 60 °C for 12–16 hours using DMF and TEA as solvent and base, respectively, and produced the title compounds QS(1–12)[41] with excellent percentage yield. All intermediates and title compounds have more than 90% yield. All Intermediates and final products were well purified using column chromatography with a mixer of 1 : 9 methanol : dichloromethane/chloroform and characterized using multi-spectroscopic techniques like ^{1}H NMR, ^{13}C NMR, and FT-IR spectroscopy. The verification of purity was established through liquid chromatography-mass spectrometry (LC-MS).

2.1.1 Infrared (IR) spectroscopy. The occurrence of distinctive peaks within the IR spectral analysis around

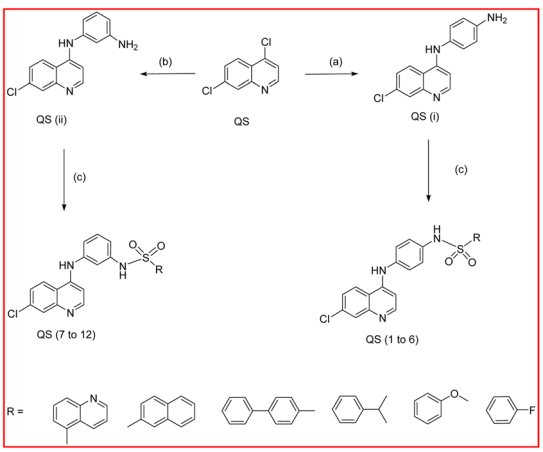

Scheme 1 Synthetic routes used for the synthesis of quinoline and sulfonamide-based hybrid molecules. Reagents and conditions: (a) *p*-phenylenediamine, *p*-TSA, EtOH, 3 h, heat; (b) *m*-phenylenediamine, *p*-TSA, EtOH, 3 h, heat; (c) substituted sulfonyl chloride, TEA, DMF, overnight.

3400 cm^{-1}, attributed to the –NH– stretching vibrations and around 1335 cm^{-1}, attributed to the S=O stretching vibrations of the sulfonamide moiety, provided conclusive evidence of the formation of the sulfonamide derivatives.

2.1.2 ^{1}H nuclear magnetic resonance (NMR) spectroscopy. The identification of benzene rings, with their peaks aligning with the anticipated region, served as the foundation for the synthesis of the desired molecule, as the presence of the sulfonamide moiety could be determined by ^{1}H NMR. The appearance of peaks within the chemical shift ranges of 10.12–10.49 ppm confirmed the presence of the sulfonamide –NH– formation. This –NH– moiety confirmed the desired product. Although, some solvent impurities occurred in few spectra at 5.77 ppm approximately of dichloro methane (CH_2) show the singlet as impurities while water and DMSO peaks also occurred in the range of 3.39 ppm and 2.50–2.52 ppm respectively.

2.1.3 ^{13}C nuclear magnetic resonance (NMR) spectroscopy. To confirm the formation of the desired compound, a ^{13}C NMR analysis was also performed, as sulfonyl was attached to benzene carbon atoms that exhibit distinctive resonances. The appearance of peaks within the chemical shift ranges of 135–138 ppm confirmed the desired compounds. The spectra identified several impurities, including signals related to solvents. Dimethyl sulfoxide (DMSO) displayed a quartet at 40.65–39.35 ppm, while dichloromethane (CH_2Cl_2) produced a singlet around 55 ppm. Other impurities detected included chloroform at approximately 79 ppm, diethyl ether near 66 ppm, and ethanol (CH_2) at around 56.07 ppm.

2.1.4 Liquid chromatography/mass spectrometry (LC/MS). Furthermore, the LCMS analysis provided critical insights into the composition and purity of the synthesized compounds. The chromatographic separation was achieved under optimized conditions, and the corresponding mass spectrometric data were recorded. The mass spectra exhibited the molecular ion peak at the mass spectra of all synthesized compounds exhibited $[M + H]^+$ and $[M - H]^-$ peaks that corresponded to their respective chemical formulas, providing further evidence of successful synthesis and the integration of peak areas indicated that the target compound represented percentage of the total chromatographic area, suggesting a high level of purity. However, minor peaks at retention times were identified as potential impurities or degradation products, all the synthesized compounds are pure (see ESI file†)

2.2 Chemical synthesis

The synthesis protocol of the reported compounds is shown in Scheme 1 as given below.

2.3 Antibacterial studies

2.3.1 *In vitro* antibacterial screening. To screen the compounds QS1–QS12, their zones of inhibition against bacterial strains, namely *Escherichia coli* (MTCC 443), *Enterococcus faecalis* (MTCC 439), *Pseudomonas aeruginosa* (MTCC 2453), and *Salmonella typhi* (ST), were measured. A clear zone of inhibition measuring 6 mm was observed against *E. coli* isolates when treated with QS1. Compound QS4 exhibited a clearance zone against *E. coli*, *E. faecalis*, and *S. typhi.* QS3 demonstrated inhibition zones against all tested isolates, proving to be highly effective and broad-spectrum, affecting both Gram-positive and Gram-negative strains (refer to Table 1). Compounds QS5 and QS7 were found effective against *P. aeruginosa* and *E. faecalis*, respectively. QS9 inhibited *E. coli* and *S. typhi.* QS3 formed a 12 mm diameter zone against *E. coli* and an 11 mm diameter zone against *S. typhi.* No zone of inhibition was observed around the discs containing compounds QS2, QS6, QS8, QS10, QS11, and QS12 against all tested isolates. Overall, among all tested compounds, QS3 exhibited significant inhibitory potential.

Table 1 *In vitro* preliminary screening of quinoline–sulfonamide hybrids (ZOI in mm)[a]

Compound	*E. coli*	*E. faecalis*	*P. aeruginosa*	*S. typhi.*
QS1	06	—	—	—
QS2	—	—	—	—
QS3	12	07	09	11
QS4	07	06	—	06
QS5	—	—	06	—
QS6	—	—	—	—
QS7	—	06	—	—
QS8	—	—	—	—
QS9	06	—	—	07
QS10	—	—	—	—
QS11	—	—	—	—
QS12	—	—	—	—
Ciprofloxacin	25	18	24	18

[a] CIP: ciprofloxacin.

2.3.2 Minimum inhibitory concentration (MIC). Building on the screening profile of the compounds, we conducted a thorough evaluation of the antibacterial potential of the selected compound QS3 by determining its Minimum Inhibitory Concentrations (MIC). MIC represents the lowest concentration of an antimicrobial agent that prevents visible growth of the microorganism. Notably, compound QS3 exhibited an MIC value of 64 μg mL^{-1} against *P. aeruginosa*, 128 μg mL^{-1} against both *E. faecalis* and *E. coli*, and 512 μg mL^{-1} against *S. typhi.* (ESI Table S1†). Consequently, the results lead to the conclusion that QS3 serves as a selective inhibitor of *P. aeruginosa* bacterial cells, showcasing superior inhibitory properties.

2.3.3 Disk diffusion assay. To assess the antibacterial efficacy of the chosen compound QS3, a disk diffusion assay was conducted using disks saturated with concentrations equivalent to $\frac{1}{2}$MIC, MIC, and 2MIC values, plated on Mueller Hinton Agar (MHA). In the case of *E. faecalis*, QS3 exhibited zones measuring 7 mm, 8 mm, and 8 mm at $\frac{1}{2}$MIC, MIC, and 2MIC, respectively. Similarly, against *S. typhi.*, it produced zone diameters of 7 mm, 7 mm, and 8 mm at $\frac{1}{2}$MIC, MIC, and 2MIC concentrations, respectively (Table 2). Furthermore, when applied to *P. aeruginosa*, QS3 resulted in zone diameters of 6 mm, 8 mm, and 10 mm at $\frac{1}{2}$MIC, MIC, and 2MIC concentrations, respectively.

2.3.4 Combination assay. To evaluate the potential synergistic, additive, or antagonistic effects of the antibacterial compound when used in conjunction with the ciprofloxacin

Table 2 Zone of inhibition (in mm) measured around the well of ½MIC, MIC and 2MIC concentration of the compound

	Zone of inhibition (in mm) at different concentrations of test compound		
Isolates	½MIC	MIC	2MIC
E. coli	06	07	07
E. faecalis	07	08	08
P. aeruginosa	06	08	10
S. typhi.	07	07	08

combination, the combination assay was performed. This helps determine whether the combination enhances antibacterial efficacy, potentially reduces the required dosage of each compound, or mitigates resistance development in target bacterial strains. The synergistic potential of QS3 in combination with standard drug ciprofloxacin was assessed against *E. coli*, *E. faecalis*, *P. aeruginosa*, and *Salmonella typhi*. QS3 compound exhibited significant synergistic effects with ciprofloxacin against *E. faecalis*, *E. coli* and *S. typhi.* resulting in many folds reduction in their combinatorial MIC values. With *P. aeruginosa* it showed an indifferent effect in combination with CIP (Table 3).

2.3.5 Evaluation of *in vitro* toxicity. The hemolytic toxicity of compound QS3 was assessed using human red blood cells (hRBCs) across a concentration range of 50 μg mL^{-1} to 1000 μg mL^{-1}. Ampicillin served as the standard drug for toxicity comparison. Notably, QS3 exhibited less than 5% RBC lysis even at the highest concentration of 1000 μg mL^{-1}, while its maximum MIC against the tested isolates was observed to be 512 μg mL^{-1} (Fig. 2). Furthermore, the compound demonstrated lower toxicity at concentrations surpassing the MIC, indicating its safety profile with negligible effects on RBCs.

2.3.6 Effect of lead compound on environmental multi-drug resistant strains. QS3 was subjected to further investigation to assess its inhibitory impact on environmentally resistant strains. The evaluation involved measuring zones of inhibition against a total of 17 distinct strains, all of which were isolated from diverse water bodies. These zones were then compared with the reference antibacterial drug, Ampicillin. Remarkably, QS3 demonstrated a heightened inhibitory effect, particularly noteworthy in the case of resistant strains AA202 and AA290. For these specific strains, QS3 exhibited an 8 mm zone of inhibition. It is pertinent to note that when compared to the standard antibacterial drug, Ampicillin, these strains displayed resistance to Ampicillin. As a result of these comparative assessments, it was concluded that QS3 surpasses the efficacy of Ampicillin. This conclusion is drawn from its ability to efficiently inhibit the growth of selectively resistant bacterial strains (ESI Table S2†). Thus, QS3 emerges as a promising antibacterial agent with notable potential in combating environmentally resistant strains.

Table 3 Synergistic effect of compound QS-3 with standard antibacterial drug ciprofloxacin

	MIC alone (μg mL^{-1})		MIC in combination (μg mL^{-1})			
Bacterial strain	Comp	CIP	Comp	CIP	FICI	Mode of interaction
E. coli	128	0.5	2	0.125	0.26	Synergistic
E. faecalis	128	0.5	2	0.125	0.26	Synergistic
P. aeruginosa	64	0.5	4	0.5	1	Indifferent
S. typhi.	512	0.5	2	0.25	0.5	Synergistic

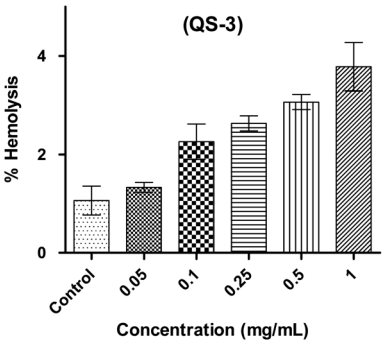

Fig. 2 Hemolytic assay of compound QS3 on human red blood cells (hRBCs) with standard drug ampicillin.

2.4 *In silico* studies

2.4.1 Prediction of physicochemical properties. In order to combat bacterial strains that exhibit resistance, the structure of quinoline–sulfonamide was focused and developed new derivatives. It is critical to evaluate the drug-like properties of these proposed compounds before synthesizing them, as poor physicochemical characteristics often lead to the failure of drugs during clinical trials. To determine these properties, Absorption, Distribution, Metabolism, and Excretion (ADME) parameters were utilized and predicted, which are summarized in ESI Table S3.† All the compounds revealed zero Lipinski violation (except QS6, & QS12), indicating that designed chemical compounds exhibit drug-like properties (see the ESI†).[42]

2.4.2 Molecular docking. We conducted blind docking in this study with the crystal structure of the putative modulator of gyrase (PmbA) from *Pseudomonas aeruginosa* (PDB ID: 3QTD) because the lead compound demonstrated significant antibacterial activity against *Pseudomonas aeruginosa* which is known for its role in various infections, particularly in immunocompromised individuals.

The binding affinities of QS-3 were determined across all four chains (A, B, C, and D) of the target protein, with the best energy observed in chain C at −8.0 kcal mol^{-1}—better than the reference drug ciprofloxacin, which had a binding energy of −7.6 kcal mol^{-1}. The molecular docking poses (A) cartoon image and (B) solid surface images show the interactions of QS-3 with Ser264 and Ser332, and ciprofloxacin with Asn209, Ala214, and Asp207, respectively (chain C). The ligPlot images (C) highlight hydrophobic interactions for QS-3 with Gly262, Leu260, Gly257, Gly346, Val327, Gly329, Tyr331, Tyr269, Arg270, Gly266, and for ciprofloxacin with Leu260, Gly257, Gly261, Gly346, Val327, Gly266, Arg270, Gly329, Tyr331, and Tyr269. QS-3 forms two hydrogen bond interactions, while ciprofloxacin forms three, as shown in Fig. 3. Additional details are provided in Table 4.

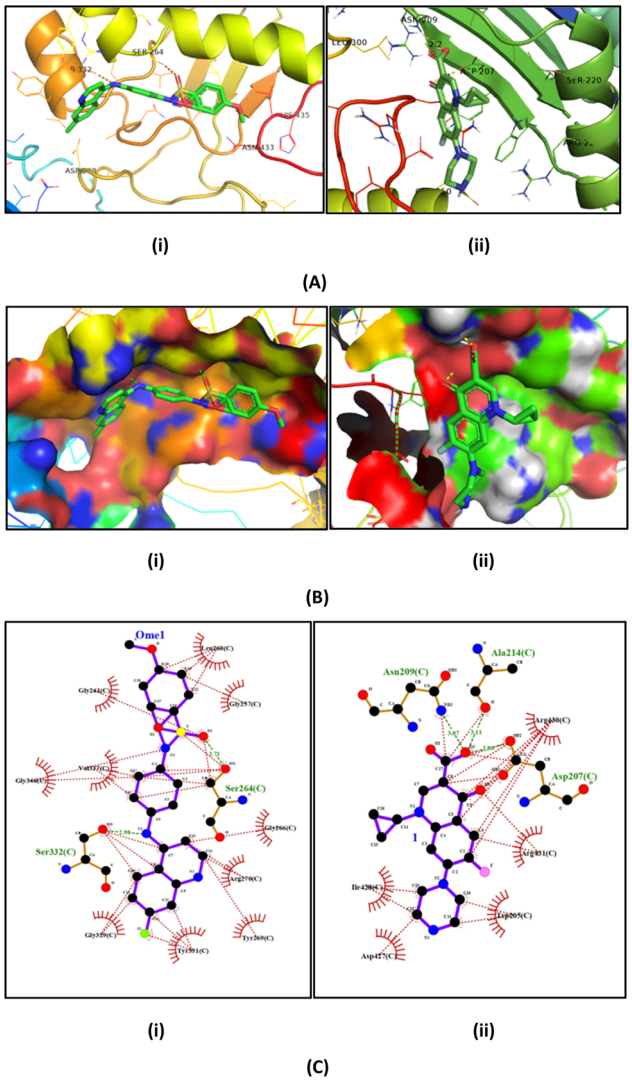

Fig. 3 Molecular docking poses with gyrase enzyme (PDB: 3QTD): (A) cartoon images (B) solid surface images of (i) QS-3 and (ii) ciprofloxacin; showing interactions with protein residues; (C) ligPlot images highlighting hydrophobic interactions (orange) and hydrogen bonds (green).

3. Experimental

The details of the experiment are given in the ESI file.† However, some important methodologies are described herein.

3.1 Chemicals and reagents

All chemicals and solvents were of analytical grade and purchased from Sigma-Aldrich, USA. The chemicals used were 4,7-dichloroquinoline *p*-phenylenediamine/*m*-phenylenediamine, *m*-phenylenediamine, substituted sulfonyl chloride, catalyst para toluene sulfonic acid (*p*-TSA) or tosylic acid (TsOH), ethanol (EtOH), triethyle amine (TEA), dimethylformamide (DMF), potassium hydroxide, methanol, sulfonyl chloride, sodium bicarbonate, sodium sulfate, brine water, dichloromethane, ethyl acetate dimethylsulfoxide (DMSO), ciprofloxacin (CIP), ampicillin (AMP), triton-X, ethylenediaminetetraacetic acid (EDTA), sodium chloride, potassium chloride, disodium hydrogen phosphate, dipotassium hydrogen phosphate and ethanol.

3.2 Instruments used

The instruments used were A digital Buchi melting point (MP) apparatus (M-560), TLC aluminum sheets of Merck silica gel 60 F254, FT-IR spectrometer of Agilent Cary 630, UV light chamber, NMR of Bruker Spectro Spin DPX-300, spectrometer using $CDCl_3$/DMSO-d_6 as a solvent Thermo Scientific Multiskan for optical density of the cultures, Laminar air flow for aseptic condition, Orbitek Incubator Shaker (Scigenics Biotech) and LC-MS of Agilent Quadrupole-6150 LC-MS.

3.3 *In vitro* studies

3.3.1 Preparation and maintenance of bacterial isolates. The four strains of bacteria used were *Escherichia coli* (MTCC 443), *Enterococcus faecalis* (MTCC 439), *Pseudomonas aeruginosa* (MTCC 2453), and *Salmonella typhi* (ST). These strains were streaked on nutrient agar plates and maintained overnight at 37 °C in an incubator.[41] A single, pure colony of each strain was selected, inoculated into nutrient broth taken in test tube, and cultivated overnight in an incubator shaker to obtain the primary culture. Inoculation was done from primary culture into different set of test tubes to get the secondary culture that were used in all the experiments.[43]

3.3.2 *In vitro* antibacterial screening of synthesized compounds. *In vitro* screening of 12 compounds of QS series named QS1–QS12 was performed to determine their antibacterial efficacies by measuring the zones of inhibition formed against the seven bacterial strains *i.e.*, *E. coli*, *E. faecalis*, *P. aeruginosa* and *S. typhi.* All the twelve compounds were dissolved in medical grade DMSO (dimethyl sulfoxide) to prepare

Table 4 Molecular docking and ligplot study of lead compound QS3 interaction with target protein

Compound	Target (PDB code)	Binding affinities (kcal mol^{-1})	No. of H-bonds	H-bond length (Å)	Residue involved in H-bonds	Residue involved in hydrophobic interaction
QS3	Putative modulator of gyrase (PmbA) from *Pseudomonas aeruginosa* (PDB ID: 3QTD)	−8.00	2	2.71 2.98	Ser 264 Ser 332	Gly262, Leu260, Gly257, Gly346, Val327, Gly329, Tyr331, Tyr269, Arg270, Gly266
Ciprofloxacin		−7.6	3	307 311 280	Asn209 Ala214 Asp207	Leu260, Gly257, Gly261, Gly346, Val327, Gly266, Arg270, Gly329, Tyr331, Try269

10 mg mL^{-1} stock solutions and sterile paper disks were allowed to soak in respective compound's solution. 50 μL of each strain (about 105 CFU mL^{-1}) was spread uniformly on Petri plates containing Mueller Hinton Agar (MHA) using sterile glass beads. The Petri plates were labelled earlier indicating the respective strain and the names of compounds. After spreading, the disks drenched with individual compounds were placed onto the agar at their respective spots using sterile forceps. For control, disks saturated with standard antibiotic ciprofloxacin (CIP) and the solvent DMSO along with an unsoaked disk (Blank) were used. Once all the disks had been placed, the plates were sealed with parafilm and incubated inverted overnight at 37 °C. The next day, the plates were observed for the presence of zones of inhibition around the disks and their diameters of zones were measured.[44]

3.3.3 Minimum inhibitory concentration (MIC). The MIC value of selected compound QS3 against the above-mentioned bacterial strains was determined. 10 mg mL^{-1} stock solutions of the compounds and 0.64 mg mL^{-1} stock solution of standard drug ciprofloxacin dissolved in DMSO were prepared. In a 96-well plate, compounds were added to nutrient broth contained in the wells such that the highest concentration of 1024 μg mL^{-1} was achieved in the first row. By performing progressive serial dilutions horizontally using a multichannel pipette, a gradient of logarithmic concentrations starting from 1024 μg mL^{-1} to 2 μg mL^{-1} was attained. In each well, 10 μl of bacterial culture (about 2 × 105 CFU mL^{-1}) was inoculated. Positive control and negative control were also included. These plates were incubated overnight at 37 °C in an incubator shaker at 90 rpm. Later, the bacterial growth was measured turbidimetrically at 590 nm using a spectrophotometer. The MIC was determined as the lowest concentration at which no visible growth was observed.[1–3,45]

3.3.4 Disk diffusion assay. Disks impregnated with test compound QS3 of concentrations equivalent to their $\frac{1}{2}$MIC, MIC and 2MIC values were placed on Mueller Hinton Agar (MHA) plates containing a uniform spread of aforementioned bacterial inoculum. Ciprofloxacin was used as the reference drug. These plates were then incubated overnight at 37 °C. After incubation, their respective zones of inhibition (ZOI) were measured in millimetres (mm) and analysed.[46] These measurements were then compared to the ZOI exhibited by the positive and negative controls, providing insights into the antimicrobial potential of the selected compounds.

3.3.5 Combination assay. Compound QS3 was evaluated for their synergistic activity in combination with standard drug ciprofloxacin using microdilution checkerboard method.[47] In a 96-well plate containing nutrient broth, CIP was diluted horizontally to achieve concentrations of 16, 8, 4, 2, 1, 0.5, 0.25, 0.125, 0.062 and 0.031 μg mL^{-1}. Then, test compound was serially diluted vertically to achieve concentrations of 256, 128, 64, 32, 16, 8, 4 and 2 μg mL^{-1} in order to form 80 combinations. 15 μl of bacterial culture (about 2 × 10 5 CFU mL^{-1}) was inoculated in each well and were incubated overnight at 37 °C in an incubator shaker at 90 rpm. After incubation, the bacterial growth was measured at 590 nm using a spectrophotometer. The wells showing no visible growth were considered as the MIC values in combination. The synergy of compound was determined in terms of FICI (fractional inhibitory concentration index) using the equation below. FICI value ≤0.5 indicated synergy, FICI value between 0.5 and 4 showed indifference and value ≥4 indicated antagonism.

$$\mathrm{FICI} = \frac{\text{MIC of drug A in combination with B}}{\text{MIC of drug A alone}} + \frac{\text{MIC of drug B in combination with A}}{\text{MIC of drug B alone}}$$

3.3.6 Haemolytic assay. The haemolytic assay was conducted utilizing the lead compound QS3. Human blood was taken from a healthy person and collected in anticoagulant tubes containing EDTA. The erythrocytes (red blood cells) were then subjected to centrifugation at 2000 rpm and 20 °C for duration of 10 minutes. Following this, the harvested erythrocytes underwent a thorough washing process with phosphate buffered saline (PBS), which was repeated three times. Subsequently, PBS was added to the resulting pellet to create a 10% erythrocytes/PBS suspension (volume/volume). The 10.0% suspension was further diluted in PBS at a ratio of 1 : 10. From each diluted suspension, 100.0 μL was added in triplicate to 100.0 μL of various dilution series of test compounds present in micro-centrifuge tubes containing the same buffer solution. 1.0% Triton X-100 was used to attain complete haemolysis. The tubes were then placed in an incubator at 37 °C for duration of one hour, followed by centrifugation at 2000 rpm for 10.0 minutes at 20.0 °C. 150.0 μL of the resultant supernatant was transferred to a flat-bottomed Tarson microtiter plate, and the absorbance was measured. at a wavelength of 450 nm using a spectrophotometer.[48]

$$\%\ \text{Hemolysis} = [(A - B)/(C - B)] \times 100$$

whereas: A = OD (optical density) of the treated sample at 450 nm B = OD of the blank (buffer) at 450 nm C = OD of the sample treated with 1% Triton X (control) at 450 nm.

3.3.7 Molecular docking. Molecular modeling simulation is a powerful computational technique used to evaluate the binding energy and interactions of antagonists with the binding site of a targeted receptor. In this study, comprehensive *in silico* molecular docking simulations were conducted to gain insights into the interaction mode of the *N*-(4-((7-chloroquinolin-4-yl) amino)phenyl)-4-methoxybenzenesulfonamide (QS-3) conjugate with the DNA gyrase enzyme, specifically focusing on its interaction with protein residues and structural features.

The molecular modeling studies followed a well-established protocol using various software tools, including ChemDraw Professional 16.0, AutoDock Tools 1.5.6, AutoDock Vina 4.0, Discovery Studio, PyMOL and Ligplot. The crystal structure of the putative modulator of gyrase (PmbA) from *Pseudomonas aeruginosa* (PDB ID: 3QTD), obtained from the Protein Data Bank, served as the target protein. The PDB files for the selected X-ray structures were sourced from the protein database. The 2D structures were generated using ChemDraw software. The PDB file for Ligand preparation involved converting these

structures into energy-minimized 3D models with Chem3D 16.0. The undesired molecules were removed from the gyrase protein using Discovery Studio, and a grid box was created using AutoDock Tools. The coordinates of compound QS-3 and ciprofloxacin were center_x = 37.702, center_y = 2.534, center_z = 160.609 and center_x = 37.927, center_y = 0.119, center_z = 160.682 respectively. The binding affinities were calculated using AutoDock Vina 4.0, and the 3D visualization of results was accomplished with PyMOL. The Ligplot was used for generating structures to analyse hydrophilic and hydrophobic interaction with amino acid residues. The resulting conformations, including 3D cartoon and solid surface poses of QS-3 and ciprofloxacin were analyzed to assess their interactions with amino acid residues and evaluate their binding energies. All the software used in this study were freeware.[49,50]

3.4 General procedure

3.4.1 Procedure for the synthesis of 4-anilinoquinoline QS-(i) & QS-(ii). A solution of 4,7-dichloroquinoline (1.0 equiv.) and *p*-phenylenediamine or *m*-phenylenediamine (2.0 equiv.) in absolute ethanol was refluxed in presence of *p*-TSA as a catalyst for 3 h. During the refluxing, precipitation of product occurred. The precipitate was collected through filtration, washed with ethanol and dried under vacuum to get the desired 4-anilinoquinoline QS-(i) & QS-(ii) with excellent yields.

3.4.1.1 N-(7-Chloro-quinolin-4-yl)-benzene-1,4-diamine QS-(i). Yellow powder, yield: 94%; mp > 211 °C; MS: 270 (M + 1); ^{1}H NMR (300 MHz, DMSO-d_6): d 8.54 (d, 1H, J = 5.31 Hz, Ar–H), 8.04 (d, 1H, J = 2.04 Hz, Ar–H), 8.85 (d, 1H, J = 8.97 Hz, Ar–H), 7.54 (d, 2H, J = 8.74 Hz, Ar–H), 7.49 (dd, 1H, J = 2.04, 8.97 Hz, Ar–H), 7.10 (d, 2H, J = 8.74 Hz, Ar–H), 6.83 (d, 1H, J = 5.31, Ar–H).

3.4.1.2 N-(7-Chloro-quinolin-4-yl)-benzene-1,3-diamine QS-(ii). Yellow greenish powder, yield: 92%; mp 206–207 °C; MS: 270 (M + 1); 1H NMR (300 MHz, DMSO-d_6): d 8.56 (d, 1H, J = 5.32 Hz, Ar–H), 8.06 (d, 1H, J = 1.98 Hz, Ar–H), 7.94 (s, 1H, Ar–H), 7.87 (d, 1H, J = 8.94 Hz, Ar–H), 7.44 (dd, 1H, J = 1.98, 8.94 Hz, Ar–H), 7.34 (t, 1H, J = 7.98 Hz, Ar–H), 7.18 (d, 1H, J = 7.21 Hz, Ar–H), 6.96 (d, 1H, J = 7.22 Hz, Ar–H), 6.89 (d, 1H, J = 5.32 Hz, Ar–H).

3.4.2 Procedure for the synthesis of 4-anilinoquinolines QS-(1–12). The appropriate sulfonyl chloride (1.2 mmol) was treated with the respective *N*-(7-chloro-quinolin-4-yl)-benzene-1,4-diamine QS-(i) and *N*-(7-chloro-quinolin-4-yl)-benzene-1,3-diamine QS-(ii) (1 mmol) in DMF as solvent and TEA used as a base (1 mmol). The reaction mixture was kept under stirring at 25 °C for 24 h and was poured into ice cold water (50 mL). The precipitate was filtered and dried. The residual crude product was purified *via* silica gel column chromatography using a gradient mixture of hexane/ethyl acetate. Compounds 1–12 were obtained as white solids with an excellent yield of 85–92%.

3.4.2.1 N-(4-((7-Chloroquinolin-4-yl)amino)phenyl)quinoline-5-sulfonamide (QS-1). Greenish yellow powder, mp: 248 °C, yield: 85%, Rf (5% MeOH in DCM): 0.41, FTIR-3249, 3059, 1976, 1994, 1618, 1547, 1570, 1514, 1331.1149. ^{1}H NMR (400 MHz, DMSO d_6) δ 10.12 (s, 1H), 9.19 (dd, J = 4.2, 1.8 Hz, 1H), 8.92 (s, 1H), 8.54 (dd, J = 8.4, 1.8 Hz, 1H), 8.42–8.24 (m, 4H), 7.85 (d, J = 2.2 Hz, 1H), 7.79–7.69 (m, 2H), 7.51 (dd, J = 9.0, 2.3 Hz, 1H), 7.11 (s, 4H), 6.62 (d, J = 5.4 Hz, 1H). ^{13}C NMR (101 MHz, DMSO d_6) δ 152.20, 151.96, 149.73, 148.62, 143.21, 137.50, 136.36, 135.69, 134.71, 134.49, 134.36, 132.60, 128.87, 127.93, 126.14, 125.31, 124.73, 124.18, 123.15, 121.83, 118.44, 101.70. Chemical formula: $C_{24}H_{17}ClN_4O_2S$, exact mass: 460.0761, MS: 461.15 $[M + H]^+$.

3.4.2.2 N-(4-((7-Chloroquinolin-4-yl)amino)phenyl)-4-fluorobenzenesulfonamide (QS-2). Whitish crystalline powder, mp: 245 °C, yield: 91%, Rf (5% MeOH in DCM): 0.39, FTIR-3368, 2981, 1741, 1618, 1577, 1514, 1331, 1238, 1167; ^{1}H NMR (400 MHz, DMSO d_6) δ 10.30 (s, 1H), 9.03 (s, 1H), 8.43 (d, J = 5.3 Hz, 1H), 8.38 (d, J = 9.0 Hz, 1H), 7.91–7.79 (m, 3H), 7.56 (dd, J = 9.0, 2.3 Hz, 1H), 7.49–7.38 (m, 2H), 7.30–7.22 (m, 2H), 7.19–7.11 (m, 2H), 6.77 (d, J = 5.4 Hz, 1H); ^{13}C NMR (101 MHz, DMSO d_6) δ 166.03, 163.53, 152.39, 149.96, 148.49, 137.16, 136.29, 136.26, 134.36, 133.93, 130.29, 130.19, 128.10, 125.37, 124.80, 124.26, 122.64, 118.62, 117.04, 116.81, 101.96. Chemical formula: $C_{21}H_{15}ClFN_3O_2S$, exact mass: 427.0558, MS: 428.11 $[M + H]^+$.

3.4.2.3 N-(4-((7-Chloroquinolin-4-yl)amino)phenyl)-4-methoxybenzenesulfonamide (QS-3). Yellowish cream crystalline powder, mp: 234 °C, yield: 92%, Rf (5% MeOH in DCM): 0.42, FTIR-3368, 2925, 1741, 1581, 1331, 1261, 1156. ^{1}H NMR (400 MHz, DMSO d_6)10.14 (s, 1H), 9.01 (s, 1H), 8.45–8.30 (m, 2H), 7.88 (d, J = 2.3 Hz, 1H), 7.75–7.67 (m, 2H), 7.55 (dd, J = 9.0, 2.3 Hz, 1H), 7.28–7.20 (m, 2H), 7.18–7.10 (m, 2H), 7.13–7.04 (m, 2H), 6.74 (d, J = 5.4 Hz, 1H), 3.81 (s, 3H); ^{13}C NMR (101 MHz, DMSO d_6) δ 162.87, 152.37, 149.94, 148.60, 136.67, 134.52, 134.35, 131.60, 129.38, 128.08, 125.34, 124.80, 124.36, 122.12, 118.57, 114.82, 101.85, 56.10. Chemical formula: $C_{22}H_{18}ClN_3O_3S$, exact mass: 439.0757, MS: 440.18 $[M + H]^+$.

3.4.2.4 N-(4-((7-Chloroquinolin-4-yl)amino)phenyl) naphthalene-2-sulfonamide (QS-4). Yellowish crystalline powder, mp: 232 °C, yield: 92%, Rf (5% MeOH in DCM): 0.41, FTIR-3379, 3041, 2981, 1737, 1577, 1514, 1331, 1235, 1160. ^{1}H NMR (400 MHz, DMSO d_6) δ 10.39 (s, 1H), 8.98 (s, 1H), 8.45 (s, 1H), 8.41–8.31 (m, 2H), 8.14 (t, J = 9.2 Hz, 2H), 8.03 (d, J = 8.0 Hz, 1H), 7.90–7.79 (m, 3H), 7.75–7.62 (m, 1H), 7.53 (dd, J = 9.1, 2.3 Hz, 1H), 7.25–7.15 (m, 4H), 6.69 (d, J = 5.4 Hz, 1H); ^{13}C NMR (101 MHz, DMSO d_6) δ 170.80, 152.32, 149.91, 148.54, 136.92, 134.72, 134.33, 134.20, 132.02, 129.89, 129.70, 129.43, 128.47, 128.31, 128.16, 128.06, 125.32, 124.77, 124.35, 122.57, 122.45, 118.54, 101.85, chemical formula: $C_{25}H_{18}ClN_3O_2S$, exact mass: 459.0808, MS: 460.08 $[M + H]^+$.

3.4.2.5 N-(4-((7-Chloroquinolin-4-yl)amino)phenyl)-4-isopropylbenzenesulfonamide (QS-5). Yellow powder, mp: 228 °C, yield: 92%, Rf (5% MeOH in DCM): 0.42, FTIR-3387, 3061, 2970, 1748, 1581, 1510, 1331, 1156. ^{1}H NMR (400 MHz, DMSO d_6) δ 10.26 (s, 1H), 9.01 (s, 1H), 8.44–8.34 (m, 2H), 7.88 (d, J = 2.3 Hz, 1H), 7.75–7.68 (m, 2H), 7.55 (dd, J = 9.1, 2.3 Hz, 1H), 7.48–7.40 (m, 2H), 7.28–7.20 (m, 2H), 7.20–7.12 (m, 2H), 6.74 (d, J = 5.4 Hz, 1H), 2.95 (hept, J = 7.1 Hz, 1H), 1.19 (d, J = 6.9 Hz, 6H); ^{13}C NMR (101 MHz, DMSO d_6) δ 154.09, 152.36, 149.95, 148.59, 137.60, 136.65, 134.44, 134.34, 128.10, 127.64, 127.32, 125.34, 124.79, 124.39, 121.93, 118.57, 101.84, 60.23, 40.60,

33.79, 23.87 (s), chemical formula: $C_{24}H_{22}ClN_3O_2S$, exact mass: 451.1121, MS: 452.26 $[M + H]^+$.

3.4.2.6 N-(4-((7-Chloroquinolin-4-yl)amino)phenyl)–[1,1′-biphenyl]-4-sulfonamide (QS-6). Yellow crystalline powder, mp: 236 °C, yield: 92%, Rf (5% MeOH in DCM): 0.42, FTIR-3346, 3067, 2985, 1734, 1577, 1510, 1331, 1164. ^{1}H NMR (400 MHz, DMSO d_6) δ 10.35 (s, 1H), 9.03 (s, 1H), 8.43–8.33 (m, 2H), 7.87 (d, J = 4.1 Hz, 4H), 7.73 (d, J = 8.5 Hz, 1H), 7.58–7.48 (m, 2H), 7.50–7.41 (m, 1H), 7.26 (d, J = 9.0 Hz, 2H), 7.19 (d, J = 9.0 Hz, 2H), 6.75 (d, J = 5.4 Hz, 1H); ^{13}C NMR (101 MHz, DMSO d_6) δ 152.31 (s), 149.85 (s), 148.58 (s), 144.72 (s), 138.76 (d, J = 6.4 Hz), 136.87 (s), 134.30 (d, J = 15.2 Hz), 129.60 (s), 127.86 (s), 127.53 (s), 125.37 (s), 124.80 (s), 124.35 (s), 122.23 (s), 118.57 (s), chemical formula: $C_{27}H_{20}ClN_3O_2S$, exact mass: 485.0965, MS: 486.10 $[M + H]^+$.

3.4.2.7 N-(3-((7-Chloroquinolin-4-yl)amino)phenyl)quinoline-5-sulfonamide (QS-7). Greenish yellow powder, mp: 246 °C, yield: 92%, Rf (5% MeOH in DCM): 0.42, FTIR-3246, 3067, 2970, 1618, 1577, 1510, 1328, 1223, 1149. ^{1}H NMR (400 MHz, DMSO d_6) δ 10.12 (s, 2H), 9.18 (d, J = 6.1 Hz, 2H), 8.96 (s, 1H), 8.55 (d, J = 8.4 Hz, 2H), 8.41–8.26 (m, 9H), 7.85 (d, J = 2.3 Hz, 2H), 7.79–7.69 (m, 4H), 7.52 (dd, J = 9.1, 2.3 Hz, 2H), 7.10 (s, 8H), 6.61 (d, J = 5.4 Hz, 2H); ^{13}C NMR (101 MHz, DMSO d_6) δ 152.02, 151.96, 149.51, 148.76, 143.21, 137.50, 136.27, 135.69, 134.72, 134.57, 134.46, 132.60, 128.88, 127.75, 126.14, 125.37, 124.76, 124.24, 123.15, 121.81, 118.39, 101.68. Chemical formula: $C_{24}H_{17}ClN_4O_2S$, exact mass: 460.076, MS: 461.06 $[M + H]^+$.

3.4.2.8 N-(3-((7-Chloroquinolin-4-yl)amino)phenyl)-4-fluorobenzenesulfonamide (QS-8). Yellow crystalline powder, mp: 246 °C, yield: 89%, Rf (5% MeOH in DCM): 0.39, FTIR-3391, 2921, 2854, 1741, 1577, 1510, 1331, 1242, 1153. ^{1}H NMR (400 MHz, DMSO d_6) δ 10.42 (s, 1H), 9.12 (s, 1H), 8.42 (dd, J = 29.0, 7.2 Hz, 2H), 7.91 (d, J = 2.2 Hz, 1H), 7.86 (dd, J = 8.9, 5.1 Hz, 2H), 7.58 (dd, J = 9.0, 2.2 Hz, 1H), 7.46 (t, J = 8.8 Hz, 2H), 7.29 (t, J = 8.1 Hz, 1H), 7.12 (s, 1H), 7.04 (d, J = 8.0 Hz, 1H), 6.89 (d, J = 8.0 Hz, 1H), 6.73 (d, J = 5.3 Hz, 1H). ^{13}C NMR (101 MHz, DMSO d_6) δ 166.11, 163.61, 152.25, 150.03, 147.97, 141.52, 138.94, 136.22, 136.19, 134.49, 130.67, 130.29, 130.19, 128.14, 125.55, 125.01, 118.91, 118.52, 117.17, 116.95, 116.13, 114.08, 102.59, chemical formula: $C_{21}H_{15}ClFN_3O_2S$, exact mass: 427.0558, MS: 428.07 $[M + H]^+$.

3.4.2.9 N-(3-((7-Chloroquinolin-4-yl)amino)phenyl)-4-methoxybenzenesulfonamide (QS-9). Yellowish cream, crystalline powder, mp: 226 °C, yield: 88%, Rf (5% MeOH in DCM): 0.41, FTIR-3379, 2925, 1599, 1577, 1328, 1257, 1157. ^{1}H NMR (400 MHz, DMSO d_6) δ 10.25 (s, 1H), 9.10 (s, 1H), 8.46–8.35 (m, 2H), 7.90 (d, J = 2.3 Hz, 1H), 7.72 (d, J = 9.0 Hz, 2H), 7.57 (dd, J = 9.0, 2.3 Hz, 1H), 7.27 (t, J = 8.1 Hz, 1H), 7.10 (d, J = 2.1 Hz, 1H), 6.69 (d, J = 5.4 Hz, 1H), 3.81 (s, 3H); ^{13}C NMR (101 MHz, DMSO d_6) δ 162.98, 152.23, 150.00, 148.02, 141.36, 139.34, 134.48, 131.48, 130.57, 129.38, 128.11, 125.53, 125.01, 118.87, 118.22, 115.89, 114.94, 113.78, 102.54, 56.15, chemical formula: $C_{22}H_{18}ClN_3O_3S$, exact mass: 439.0757, MS: 440.25 $[M + H]^+$.

3.4.2.10 N-(3-((7-Chloroquinolin-4-yl)amino)phenyl)-4-isopropylbenzenesulfonamide (QS-10). White crystalline powder, mp: 227 °C, yield: 91%, Rf (5% MeOH in DCM): 0.41, FTIR-3383, 3074, 3029, 2966, 1607, 1577, 1477, 1324, 1156. ^{1}H NMR (400 MHz, DMSO d_6) δ 10.50 (s, 1H), 9.07 (s, 1H), 8.48 (s, 1H), 8.34 (d, J = 9.1 Hz, 1H), 8.15 (dd, J = 6.8, 4.3 Hz, 3H), 8.05 (d, J = 7.8 Hz, 1H), 7.92–7.78 (m, 2H), 7.78–7.63 (m, 2H), 7.55 (dd, J = 9.0, 2.2 Hz, 1H), 7.27 (t, J = 8.1 Hz, 1H), 7.12 (t, J = 1.9 Hz, 1H), 6.97 (t, J = 7.8 Hz, 2H), 6.51 (d, J = 5.3 Hz, 1H). ^{13}C NMR (101 MHz, DMSO d_6) δ 152.06, 149.94, 147.94, 141.36, 139.02, 136.83, 134.77, 134.47, 132.07, 130.64, 130.02, 129.73, 129.55, 128.48, 128.37, 128.27, 128.07, 125.52, 124.96, 122.49, 118.81, 118.54, 116.30, 114.10, 102.32, chemical formula: $C_{25}H_{18}ClN_3O_2S$, exact mass: 459.0808, MS: 460.25 $[M + H]^+$.

3.4.2.11 N-(3-((7-Chloroquinolin-4-yl)amino)phenyl)-4-isopropylbenzenesulfonamide (QS-11). Creamish white powder, mp: 222 °C, yield: 87%, Rf (5% MeOH in DCM): 0.41, FTIR-3372, 3031, 1607, 1577, 1328, 1265, 1156. 1H NMR (400 MHz, DMSO d_6) δ 10.39 (s, 1H), 9.11 (s, 1H), 8.42 (dd, J = 24.4, 7.2 Hz, 2H), 7.91 (d, J = 2.2 Hz, 1H), 7.74 (d, J = 8.4 Hz, 2H), 7.57 (dd, J = 9.0, 2.2 Hz, 1H), 7.47 (d, J = 8.4 Hz, 2H), 7.27 (t, J = 8.1 Hz, 1H), 7.15 (s, 1H), 7.01 (d, J = 8.0 Hz, 1H), 6.91 (d, J = 8.0 Hz, 1H), 6.74 (d, J = 5.3 Hz, 1H), 2.95 (hept, J = 6.9 Hz, 1H), 1.18 (d, J = 6.9 Hz, 6H). ^{13}C NMR (101 MHz, DMSO d_6) δ 154.24, 152.25, 150.04, 147.95, 141.45, 139.30, 137.52, 134.48, 130.60, 128.13, 127.75, 127.31, 125.53, 125.01, 118.9, 118.04, 115.47, 113.34, 102.60, 33.80, 23.85, chemical formula: $C_{24}H_{22}ClN_3O_2S$, exact mass: 451.1121 MS: 452.26 $[M + H]^+$.

3.4.2.12 (3-((7-Chloroquinolin-4-yl)amino)phenyl)–[1,1′-biphenyl]-4-sulfonamide (QS-12). Cream powder, mp: 225 °C, yield: 87%, Rf (5% MeOH in DCM): 0.41, FTIR-3372, 3009, 1603, 1577, 1480, 1331, 1156. ^{1}H NMR (400 MHz, DMSO d_6) δ 10.49 (s, 1H), 9.24 (s, 2H), 8.40 (d, J = 9.0 Hz, 2H), 7.95–7.85 (m, 7H), 7.73 (d, J = 8.9 Hz, 3H), 7.60 (t, J = 11.6 Hz, 1H), 7.50 (t, J = 7.4 Hz, 3H), 7.49–7.40 (m, 1H), 7.31 (t, J = 8.1 Hz, 2H), 7.17 (s, 1H), 7.04 (d, J = 5.8 Hz, 1H), 6.96 (d, J = 8.0 Hz, 1H), 6.72 (d, J = 5.5 Hz, 2H); ^{13}C NMR (101 MHz, DMSO d_6) δ 172.51, 151.69, 149.33, 148.41, 144.85, 141.31, 139.17, 138.66, 134.77, 130.72, 129.62, 129.40, 129.12, 127.95, 127.87, 127.59, 127.54, 127.19, 126.62, 126.47, 125.69, 125.09, 118.75, 118.47, 116.07, 113.89, 102.47, chemical formula: $C_{27}H_{20}ClN_3O_2S$, exact mass: 485.0965, MS: 486.23 $[M + H]^+$.

4. Conclusions

In summary, a series of quinoline–sulfonamide hybrids compounds with a substituted core was synthesized in a laboratory setting and investigated for their antibacterial properties. These compounds underwent testing on both Gram-positive bacterial strains, specifically *E. faecalis*, and Gram-negative strains, namely *E. coli*, *P. aeruginosa*, and *S. typhi.* Following a sequence of experiments to evaluate the antibacterial activity of the compounds, QS3 emerged as a promising antibacterial agent. Notably, when studied in combination with Ciprofloxacin (CIP), QS3 exhibited a synergistic nature against *E. faecalis*, *E. coli*, and *S. typhi.* Consequently, it is evident that QS3 holds the potential for further development as a safe and effective antibacterial agent.

Data availability

A data generated or analysed in this study are included in this article.

Author contributions

MA, IA and AA: conceptualized and designed the study. ZS: synthesize the compounds. IH and AA: performed *in vitro* studies. ZS, IH and AA: wrote the original draft. MA, MK, AA and IA: reviewed and edited the manuscript. MK, AA and MA: proofread the draft. All authors have read and approved the final version of the manuscript.

Conflicts of interest

The authors declared no conflict of interest.

Acknowledgements

Mohammad Abid gratefully acknowledges the financial support in the form of Core Research Grant from Science & Engineering Research Board (SERB), Govt. of India (Project No. CRG/2018/003967). Zohaib Saifi acknowledges the financial support from the University Grants Commission (UGC), Govt. of India in the form of non-NET Fellowship (UGC-Ref. No. 108/(CSIR-UGC NET DEC.2017)). Asghar Ali acknowledges the Department of Health (DHR), Govt. of India Project (File No. R.12014/61/2022-HR). M. K. also acknowledges the SERB-CRG grant (Project No. CRG/2022/003895).).

References

1 T. Xu, X. Yan, A. Kang, L. Yang, X. Li, Y. Tian, R. Yang, S. Qin and Y. Guo, *J. Med. Chem.*, 2024, **67**, 9302–9317.
2 EClinicalMedicine, *EClinicalMedicine*, 2021, **41**, 101221.
3 K. Sado, K. Keenan, A. Manataki, M. Kesby, M. F. Mushi, S. E. Mshana, J. R. Mwanga, S. Neema, B. Asiimwe, J. Bazira, J. Kiiru, D. L. Green, X. Ke, A. Maldonado-Barragán, M. Abed Al Ahad, K. J. Fredricks, S. H. Gillespie, W. Sabiiti, B. T. Mmbaga, G. Kibiki, D. Aanensen, V. A. Smith, A. Sandeman, D. J. Sloan and M. T. G. Holden, *PLoS Glob. Public Health*, 2024, **4**, e0002709.
4 C. Maria, A. M. de Matos and A. P. Rauter, *Curr. Opin. Chem. Biol.*, 2024, **78**, 102419.
5 F. Li, J. G. Collins and F. R. Keene, *Chem. Soc. Rev.*, 2015, **44**, 2529–2542.
6 I.-A. Lungu, O.-L. Moldovan, V. Biriş and A. Rusu, *Pharmaceutics*, 2022, **14**, 1749.
7 M. Hilf, V. L. Yu, J. Sharp, J. J. Zuravleff, J. A. Korvick and R. R. Muder, *Am. J. Med.*, 1989, **87**, 540–546.
8 G. Dhanda, Y. Acharya and J. Haldar, *ACS Omega*, 2023, **8**, 10757–10783.
9 S. M. Drawz and R. A. Bonomo, *Clin. Microbiol. Rev.*, 2010, **23**, 160–201.
10 T. S. Ibrahim, A. J. Almalki, A. H. Moustafa, R. M. Allam, G. E.-D. A. Abuo-Rahma, H. I. El Subbagh and M. F. A. Mohamed, *Bioorg. Chem.*, 2021, **111**, 104885.
11 P. de Sena Murteira Pinheiro, L. S. Franco, T. L. Montagnoli and C. A. M. Fraga, *Expet Opin. Drug Discov.*, 2024, **19**, 451–470.
12 L. Drago, *Microorganisms*, 2024, **12**, 649.
13 A. I. Anwar, L. Lu, C. J. Plaisance, C. P. Daniel, C. J. Flanagan, D. M. Wenger, D. McGregor, G. Varrassi, A. M. Kaye and A. D. Kaye, *Cureus*, 2024, **16**, e54565.
14 M. P. Ambatkar, N. R. Rarokar and P. B. Khedekar, *Clin. Complement. Med. Pharmacol.*, 2023, **3**, 100102.
15 S. Akhter, O. Concepcion, A. F. de la Torre, A. Ali, A. R. Raza, R. Eman, M. Khalid, M. F. ur Rehman, M. S. Akram and H. M. Ali, *Arab. J. Chem.*, 2023, **16**, 104570.
16 A. Saxena, S. Majee, D. Ray and B. Saha, *Bioorg. Med. Chem.*, 2024, **103**, 117681.
17 B. Çiftci, S. Ökten, Ü. M. Koçyiğit, V. E. Atalay, M. Ataş and O. Çakmak, *Eur. J. Med. Chem. Res.*, 2024, **10**, 100127.
18 K. El Gadali, M. Rafya, A. El Mansouri, M. Maatallah, A. Vanderlee, A. Mehdi, J. Neyts, D. Jochmans, S. De Jonghe, F. Benkhalti, Y. S. Sanghvi, M. Taourirte and H. B. Lazrek, *Eur. J. Med. Chem.*, 2024, **268**, 116235.
19 H.-X. Li, X.-F. Luo, P. Deng, S.-Y. Zhang, H. Zhou, Y. Y. Ding, Y.-R. Wang, Y.-Q. Liu and Z.-J. Zhang, *J. Agric. Food Chem.*, 2023, **71**, 2301–2312.
20 P. Králová and M. Soural, *Eur. J. Med. Chem.*, 2024, **269**, 116287.
21 R. C. Ochu, U. C. Okoro, J. Conradie and D. I. Ugwu, *Eur. J. Med. Chem. Res.*, 2024, **10**, 100136.
22 B. D. Bax, P. F. Chan, D. S. Eggleston, A. Fosberry, D. R. Gentry, F. Gorrec, I. Giordano, M. M. Hann, A. Hennessy, M. Hibbs, J. Huang, E. Jones, J. Jones, K. K. Brown, C. J. Lewis, E. W. May, M. R. Saunders, O. Singh, C. E. Spitzfaden, C. Shen, A. Shillings, A. J. Theobald, A. Wohlkonig, N. D. Pearson and M. N. Gwynn, *Nature*, 2010, **466**, 935–940.
23 K. Douadi, S. Chafaa, T. Douadi, M. Al-Noaimi and I. Kaabi, *J. Mol. Struct.*, 2020, **1217**, 128305.
24 A. Ali, P. Hasan, M. Irfan, A. Uddin, A. Khan, J. Saraswat, R. Maguire, K. Kavanagh, R. Patel, M. C. Joshi, A. Azam, M. Mohsin, Q. M. R. Haque and M. Abid, *ACS Omega*, 2021, **6**, 27798–27813.
25 J. Yadav and C. P. Kaushik, *Synth. Commun.*, 2024, **54**, 536–552.
26 S. Konda, S. Raparthi, K. Bhaskar, R. K. Munaganti, V. Guguloth, L. Nagarapu and D. M. Akkewar, *Bioorg. Med. Chem. Lett.*, 2015, **25**, 1643–1646.
27 J. Lal, S. K. Gupta, D. Thavaselvam and D. D. Agarwal, *Eur. J. Med. Chem.*, 2013, **64**, 579–588.
28 (*a*) S.-M. Wang, G.-F. Zha, K. P. Rakesh, N. Darshini, T. Shubhavathi, H. K. Vivek, N. Mallesha and H.-L. Qin, *Medchemcomm*, 2017, **8**, 1173–1189; (*b*) S. Bano, K. Javed, S. Ahmad, I. G. Rathish, S. Singh and M. S. Alam, *Eur. J. Med. Chem.*, 2011, **46**, 5763–5768.
29 X. Ning, Y. Guo, X. Ma, R. Zhu, C. Tian, Z. Zhang, X. Wang, Z. Ma and J. Liu, *Bioorg. Med. Chem.*, 2013, **21**, 5589–5597.

30 H. B. Allen and D. A. Lee, *Curr. Med. Res. Opin.*, 1973, **1**, 547–553.
31 (*a*) X. Zhang, K. P. Rakesh, C. S. Shantharam, H. M. Manukumar, A. M. Asiri, H. M. Marwani and H.-L. Qin, *Bioorg. Med. Chem.*, 2018, **26**, 340–355; (*b*) A. Thakur, S. Manohar, C. E. Vélez Gerena, B. Zayas, V. Kumar, S. V. Malhotra and D. S. Rawat, *Med. Chem. Commun.*, 2014, **5**, 576–586.
32 H. I. Gul, M. Tugrak, H. Sakagami, P. Taslimi, I. Gulcin and C. T. Supuran, *J. Enzyme Inhib. Med. Chem.*, 2016, **31**, 1619–1624.
33 V. Akurathi, L. Dubois, S. Celen, N. G. Lieuwes, S. K. Chitneni, B. J. Cleynhens, A. Innocenti, C. T. Supuran, A. M. Verbruggen, P. Lambin and G. M. Bormans, *Eur. J. Med. Chem.*, 2014, **71**, 374–384.
34 (*a*) S. Bag, R. Tulsan, A. Sood, H. Cho, H. Redjeb, W. Zhou, H. LeVine, B. Török and M. Török, *Bioorg. Med. Chem. Lett.*, 2015, **25**, 626–630; (*b*) M. Xu, Y. Peng, L. Zhu, S. Wang, J. Ji and K. P. Rakesh, *Eur. J. Med. Chem.*, 2019, **180**, 656–672.
35 H.-X. Dai, A. F. Stepan, M. S. Plummer, Y.-H. Zhang and J.-Q. Yu, *J. Am. Chem. Soc.*, 2011, **133**, 7222–7228.
36 T. Hamaguchi, T. Hirose, H. Asakawa, Y. Itoh, K. Kamado, K. Tokunaga, K. Tomita, H. Masuda, N. Watanabe and M. Namba, *Diabetes Res. Clin. Pract.*, 2004, **66**, S129–S132.
37 Y. M. Huang, N. S. Alharbi, B. Sun, C. S. Shantharam, K. P. Rakesh and H.-L. Qin, *Eur. J. Med. Chem.*, **181**, 111566.
38 R. Gawin, E. De Clercq, L. Naesens and M. Koszytkowska-Stawińska, *Bioorg. Med. Chem.*, 2008, **16**, 8379–8389.
39 (*a*) H.-L. Qin, Z.-W. Zhang, R. Lekkala, H. Alsulami and K. P. Rakesh, *Eur. J. Med. Chem.*, 2020, **193**, 112215; (*b*) N. Boechat, L. C. S. Pinheiro, O. A. Santos-Filho and I. C. Silva, *Molecules*, 2011, **16**, 8083–8097.
40 A. Kumar, K. Srivastava, S. Raja Kumar, M. I. Siddiqi, S. K. Puri, J. K. Sexana and P. M. S. Chauhan, *Eur. J. Med. Chem.*, 2011, **46**, 676–690.
41 L. C. S. Pinheiro, N. Boechat, M. de, L. G. Ferreira, C. C. S. Júnior, A. M. L. Jesus, M. M. M. Leite, N. B. Souza and A. U. Krettli, *Bioorg. Med. Chem.*, 2015, **23**, 5979–5984.
42 A. Daina, O. Michielin and V. Zoete, *Sci. Rep.*, 2017, **7**, 42717.
43 L. J. Rather, Q. Zhou, A. Ali, Q. M. R. Haque and Q. Li, *ACS Food Sci. Technol.*, 2021, **1**, 427–442.
44 R. Sultana, A. Ali, C. Twala, R. Mehandi, M. Rana, D. Yameen, M. Abid and Rahisuddin, *J. Biomol. Struct. Dyn.*, 2023, **41**, 13724–13751.
45 R. A. Al-Qawasmeh, M. M. Abadleh, J. A. Zahra, M. M. El-Abadelah, R. Albashiti, F. Zani, M. Incerti and P. Vicini, *J. Enzyme Inhib. Med. Chem.*, 2014, **29**, 777–785.
46 S. Abass, S. Zahiruddin, A. Ali, M. Irfan, B. Jan, Q. M. R. Haq, S. A. Husain and S. Ahmad, *Curr. Microbiol.*, 2022, **79**, 223.
47 K. H. Rand, H. J. Houck, P. Brown and D. Bennett, *Antimicrob. Agents Chemother.*, 1993, **37**, 613–615.
48 I. Irfan, A. Ali, B. Reddi, M. A. Khan, P. Hasan, S. Ahmed, A. Uddin, M. Piatek, K. Kavanagh, Q. M. R. Haque, S. Singh, A. Addlagatta and M. Abid, *Antibiotics*, 2022, **11**, 1126.
49 S. M. Khirallah, H. M. M. Ramadan, A. Shawky, S. H. Qahl, R. S. Baty, N. Alqadri, A. M. Alsuhaibani, M. Jaremko, A.-H. Emwas and E. M. Saied, *Molecules*, 2022, **27**, 6271.
50 S. M. Khirallah, H. M. M. Ramadan, H. A. A. Aladl, N. O. Ayaz, L. A. F. Kurdi, M. Jaremko, S. Z. Alshawwa and E. M. Saied, *Pharmaceuticals*, 2022, **15**, 1576.